Eur J Nucl Med Mol Imaging (2007) 34:939–950
DOI 10.1007/s00259-006-0359-0

REVIEW ARTICLE

Neuronal imaging using SPECT

Shohei Yamashina · Jun-ichi Yamazaki

Published online: 1 February 2007

Abstract
Background ^{123}I-metaiodobenzylguanidine (MIBG) myocardial scintigraphy is one of only a few methods available for objective evaluation of cardiac sympathetic function at a clinical level. Disorders in cardiac sympathetic function play an important role in various heart diseases, and MIBG provides an abundance of useful information for evaluation of disease severity, prognosis, and therapeutic effects; this information is of particular value in patients with heart failure, ischemic heart diseases, or arrhythmic disorders. On the other hand, the quantitative indices for MIBG differ between institutions, and evidence has not been sufficiently well established for MIBG, compared with myocardial perfusion imaging, in ischemic heart diseases.
Review In view of these difficulties, this review provides fundamental information regarding MIBG, its usefulness for various diseases and future difficulties.

Keywords Sympathetic nervous system · Cardiac disease · ^{123}I-MIBG · SPECT · Planar

Introduction

The heart is an organ with a dense distribution of sympathetic nerves. The sympathetic nervous system plays important roles in controlling the heart rate, blood pressure, capacity to cause myocardial contraction/dilation, and coronary tonus. Hypertonia of cardiac sympathetic nerves is known to cause exacerbation of myocardial ischemia, exacerbation of heart failure, and induction of severe arrhythmia, and sympathetic functional disorders have important clinical significance in heart diseases.

^{123}I-metaiodobenzylguanidine (MIBG) myocardial scintigraphy is one of the few methods available for objective evaluation of cardiac sympathetic functions at a clinical level, and provides an abundance of information useful for the evaluation of various heart diseases. This review describes fundamental information regarding MIBG imaging and interpretation, as well as its usefulness for various diseases and future difficulties.

S. Yamashina (✉) · J.-i. Yamazaki
Department of Cardiovasular Medicine,
Toho University Omori Medical Center,
6-11-1 Omori-nishi, Ota-ku,
Tokyo 143-8541, Japan
e-mail: shohei@uhchan.com

Structure and dynamics of MIBG

MIBG, an analog of norepinephrine, was developed as a sympathetic nerve imaging agent, and reported by Wieland et al. in 1980 [1]. The structures of norepinephrine and MIBG are shown in Fig. 1.

Regarding MIBG uptake, in 1985 Tobes et al. established the uptake-1 mechanism as the core mechanism for uptake into sympathetic nerve endings [2]. In addition, MIBG was reported to be stored mainly in norepinephrine storage vesicles [3] and to be released via exocytosis [4]. In other words, MIBG and norepinephrine have the same mechanisms for uptake, storage, and release. On the other hand, in contrast to norepinephrine, MIBG is not bound to receptors on the myocardial cell membrane [5] and undergoes almost no metabolism via enzymes, including catechol-*O*-methyl transferase (COMT) and monoamine oxidase (MAO) [6]. Due to these characteristics, MIBG is retained in sympathetic nerve endings, resulting in its demonstrated excellence as an imaging agent. Figure 2 shows the dynamics of norepinephrine and MIBG.

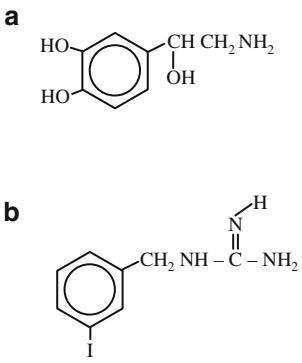

Fig. 1 Structural formulae of norepinephrine and MIBG. **a** Norepinephrine. **b** MIBG

The advent of MIBG made it possible to conduct objective in vivo evaluations of cardiac sympathetic functions. The dynamics of MIBG reflect the sympathetic activities, and thus it is possible to evaluate the local state of denervation based on the accumulation defect, and the degree of sympatheticotonia based on the washout.

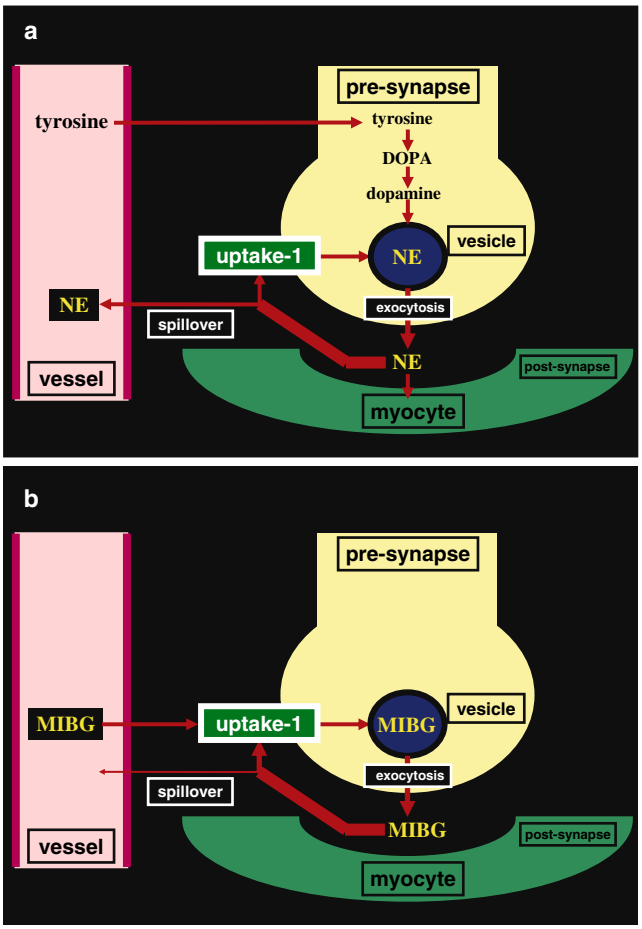

Fig. 2 Dynamics of norepinephrine and MIBG. **a**. Norepinephrine (*NE*) is stored in synaptic vesicles at sympathetic nerve endings and is released via exocytosis due to nerve excitement. Most of the released NE returns to the nerve endings via the reabsorption mechanism designated as uptake-1. A fraction of the released NE becomes bound to the receptors, while the remainder is released into the blood by spillover. The NE is ultimately inactivated by COMT and MAO. **b**. MIBG is also incorporated into nerve endings via uptake-1, and released via the excitement of nerves, in a manner similar to NE. MIBG, however, is neither bound to the receptors nor degraded by enzymes. Due to these characteristics, most of the MIBG is reabsorbed via uptake-1 and retained in the nerve ending for many hours

Imaging methods for MIBG

Before conducting the examination, it is necessary to know whether the patient has taken drugs that influence the accumulation of MIBG. It is necessary to withdraw reserpine and tricyclic antidepressant agents for an appropriate period in accordance with their blood half-lives [7]. When thyroid blocking is performed, KI powder (40–300 mg/day) is administered for 3 days from the day preceding the examination. As ^{123}I has a short half-life of 13 h and is a nuclide which emits only gamma rays, it does not necessarily require the blockage of thyroid accumulation.

MIBG 111 MBq is intravenously administered in the resting condition, and the early and delayed images are obtained 15–30 min later and 3–4 h later, respectively. It is desirable to prepare a gamma camera having a sufficient visual field to cover most of the chest, and more than two detectors. In addition, it is necessary to use a collimator for low energy or ^{123}I only, and to set the energy window to 159 keV±10%. Planar images have been used in many ways for the evaluation of cardiac sympathetic function, while SPECT images are advantageous for evaluating abnormalities in local distribution in the myocardium. In practice, both of the above images are used, in combination.

In the case of planar images, the anterior view is imaged for roughly 3–5 min, using a 128×128 or 256×256 matrix. If possible, further views in two directions are obtained at a left anterior oblique angle of 35–40° and at 70° to the left lateral plane. The SPECT images are collected using a 64×64 matrix over a 360° range, or at 180° from the right anterior oblique plane to the left posterior oblique plane. For reference, the imaging protocol at the authors' institution is shown in Fig. 3.

Analysis and interpretation of MIBG

The most common indices are the heart to mediastinum ratio (H/M ratio) and the washout rate obtained from the anterior planar images. These indices represent simple semiquantitative measures, but have been widely used, resulting in many reports which support their usefulness in the evaluation of severity and prognosis in cases of heart failure. Regions of interest (ROIs) are set over the heart (H) and the mediastinum (M) to obtain the mean count in the respective ROIs, after which the H/M ratio is calculated. Based on the ratio, the degree of accumulation in the heart is evaluated. It is desirable to set the mediastinal ROI as far as possible at an upper site

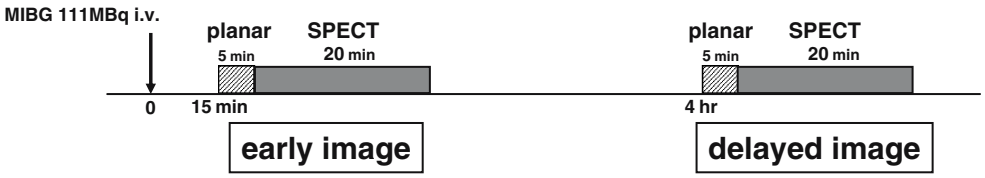

Fig. 3 One example of the MIBG imaging protocol. MIBG 111 MBq is intravenously administered under the resting condition, and the early and delayed images are obtained 15 min and 4 h later, respectively. Gamma camera, three-detector type; collimator, low energy general purpose (LEGP); energy window, 159 keV ±10%; planar image, anterior view for 5 min, 256×256 matrixes; SPECT image, 360° collection (continuous mode), non-circular orbit (near-by orbit), 64×64 matrixes, magnifying rate of collection 1.6. Pretreatment: Butterworth filter (order 8, cut-off 0.25 cycles/pixel). Reconstruction: filtered back projection (180° data, Ramp filter). One slice 3.6 mm. Neither absorption correction nor scattered ray correction

that is unaffected by the thyroid gland, and the cardiac ROI so as to surround the entire heart. The washout rate is an index that indicates the rate that MIBG is washed out between the early image and the delayed image, via comparison with the cardiac count in the early image. In this calculation, the mediastinal count is subtracted from the cardiac count as a background correction, in principle. A correction for decay due to the half-life of ^{123}I may be performed, as required. Figure 4 shows a practical method of calculating the H/M ratio and washout rate. The accumulation in the early MIBG image reflects the distribution of cardiac sympathetic nerves and the uptake-1 functions at the nerve endings, while the washout rate is an index of the degree of sympatheticotonia. The delayed image is a result of washout from the early image and thus is considered to contain combined information regarding both the accumulation in the early image and the washout rate.

Regarding the SPECT images, a method is available for visual scoring of the degree of accumulation by division into segments, which is similar to that used in myocardial perfusion imaging. The rate of uptake of MIBG in the myocardium is as low as 1–2%, and the image quality is inferior compared with ^{201}TI. In some cases, substantial accumulation of MIBG may occur in the liver, which overlaps the myocardial infero-posterior wall, and scattering from the lung field to the lateral wall then exerts a considerable influence upon the image, requiring careful interpretation.

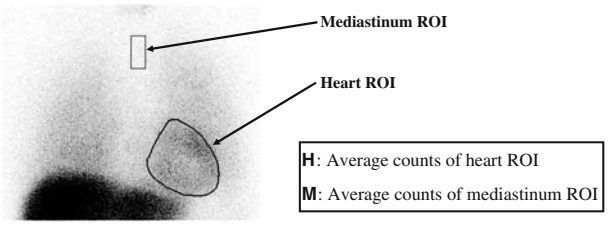

$$\text{H/M ratio} = \frac{H}{M}$$

$$\text{washout rate} = \frac{\text{early image (H - M)} - \text{delayed image (H - M)}}{\text{early image (H - M)}} \times 100\ (\%)$$

Fig. 4 Method of calculating the H/M ratio and washout rate on MIBG planar images

It is possible to obtain the relative distribution of values in respective regions from a polar map prepared using the SPECT short axis images. Even in normal cases, MIBG exhibits a relatively low uptake in the inferior wall region [8], a tendency which has been reported to become strong in the elderly [9, 10]. During interpretation, it is necessary to give careful consideration to this point. It is also possible to calculate the washout rate from the polar map, and to obtain not only a mean value for the whole left ventricle but also values for the respective regions. If a normal profile is prepared from a group of normal cases, it is possible to use the polar map to calculate extent and severity scores, which indicate the extent and severity of defects, respectively (Fig. 5).

Another quantitative index, which differs from the above indices, is the myocardial uptake rate of MIBG. One reported method of obtaining this index is as follows. First, MIBG is administered via rapid intravenous injection to obtain the dynamic data, and the rate is calculated according to the compartment model theory [11]. In another reported method, the rate is calculated from the count ratio of the myocardium and left ventricular cavity, and the radioactivity of the blood sample [12].

Ischemic heart diseases

MIBG in ischemic heart diseases

Sympathetic nerve endings are easily damaged by ischemia, in comparison with myocardial cells, and sympathetic function disorders are known to persist for a certain period even after alleviation of the ischemia. As a result, the potential exists for use of MIBG to detect ischemia with extreme sensitivity, providing images for detection of transient ischemia. Myocardial perfusion imaging as a nuclear cardiological examination has been used in many ways for ischemic heart diseases, and there is sufficient evidence regarding the usefulness of this method. However, in some cases, pathologic conditions are difficult to evaluate precisely via perfusion imaging alone, and MIBG imaging may become effective.

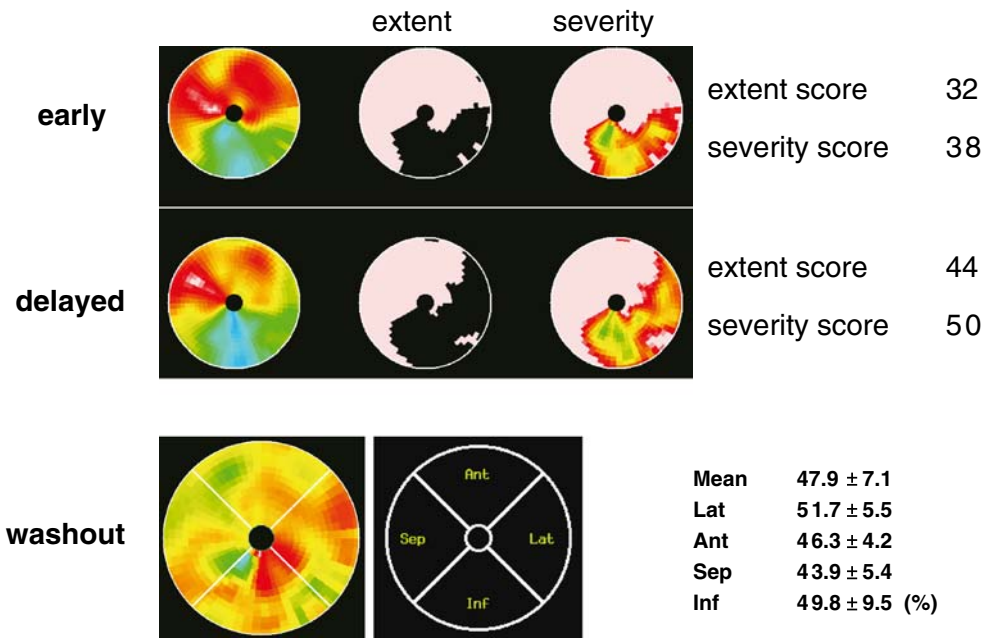

Fig. 5 Polar map analysis. In the extent map, pixels with counts of −2SD or less are displayed by blackout in comparison with the normal file prepared from normal cases, and the extent score shows the % blackout of pixels in total. In the severity map, the severity of decreased accumulation is displayed using color in terms of the blackout portion on the extent map. The severity score is the value obtained using the following formula: (the sum of the difference in counts between pixels of the blackout portion and the corresponding pixels on the normal file) / (total number of pixels). It is possible to calculate the washout rates of the various regions, in addition to the mean washout rate of the left ventricular circumference, and here mean±SD expresses the washout rates in the four divided regions

Vasospastic angina

In vasospastic angina, the practice of myocardial perfusion imaging during non-seizure results in normal accumulation, and ordinary exercise loading rarely induces coronary spasms. Accordingly, the ability of myocardial perfusion imaging to diagnose this disease is not clinically satisfactory.

According to a report by Taki et al. [13], a few cases of vasospastic angina showed abnormal early MIBG images, while a high percentage showed increased washout in the region of the culprit coronary artery on the delayed images, indicating a clearly abnormal accumulation. In other words, delayed images were highly useful for diagnosis. The positive and negative accuracy rates were favorable, at 83% and 81%, respectively. Sakata et al. [14] reported MIBG to be more useful than stress myocardial perfusion SPECT in the prediction of cardiac events in patients with vasospastic angina having no dominant coronary stenosis.

Detection of repeated ischemia is considered to be a mechanism underlying the decreased accumulation of MIBG in coronary spastic angina, although abnormal sympathetic functions may be one factor involved in the development of coronary spasm.

Unstable angina

A loading test is not indicated for unstable angina, although myocardial perfusion imaging at rest is unable to diagnose this disease in many cases. MIBG makes it possible to identify the culprit coronary artery with a high probability via findings obtained under the resting condition, indicating its diagnostic usefulness. In a study by Tsutsui et al. [15], MIBG was demonstrated to have a sensitivity of 71% and a specificity of 78% for diagnosis of the culprit coronary artery in this disease. The detection rate was reported to be high in cases in which either the period between the final seizure and the conduct of the examination was short, or the frequency of seizures was high. Figure 6 shows one case of unstable angina in which MIBG facilitated diagnosis.

Evaluation of risk areas in acute coronary syndrome

Recently, percutaneous coronary intervention (PCI) has been generally conducted for acute coronary syndrome in emergency situations. ^{99m}Tc agents are highly retained in the myocardium, and exhibit almost no redistribution phenomena, as are observed when using ^{201}TlCl. Thus, intravenous injection of such an agent prior to the practice of PCI permits evaluation of the state of myocardial perfusion before reperfusion treatment, even if the imaging is conducted after the completion of PCI (this characteristic is referred to as a freeze image). The defect range indicated on the image obtained via this method is called the risk area (i.e., the area at risk of infarction, if not treated appropriately), and is clinically important. A second myocardial perfusion imaging procedure conducted in the subacute phase makes it possible

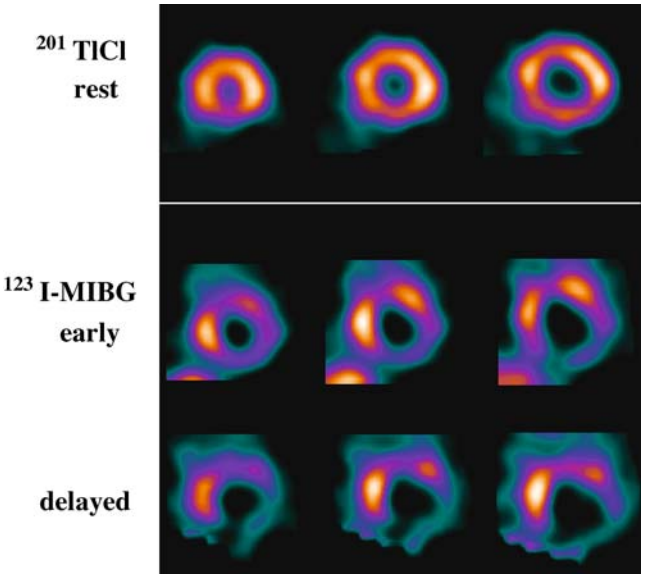

Fig. 6 A case of unstable angina in which MIBG facilitated diagnosis. Female, aged 62 years. The patient was admitted to the hospital owing to a diagnosis of unstable angina, but no significant findings were obtained via ^{201}TlCl myocardial perfusion SPECT at rest. MIBG showed decreased accumulation in the inferoposterior wall. On the delayed image, increased washout was observed at the same site, and the abnormal findings became more marked. On coronary angiography, performed later, advanced stenosis was recognized in the proximal part of the right coronary artery

to quantitatively measure the infarcted myocardium. The difference between the risk area and the infarcted area corresponds to the myocardium rescued by PCI.

While evaluation of the risk area using ^{99m}Tc agents is an excellent method with a high objectivity, it is not necessarily easy to conduct nuclear medical examinations in emergencies, during the acute phase. MIBG detects ischemia, and thus reveals a wider range of defects, if used in the subacute phase, compared with myocardial perfusion imaging; this results in a mismatch between the methods. It has been reported that the range of defects on MIBG imaging corresponds more closely to the risk area obtained using ^{99m}Tc agents [16], and MIBG is useful in evaluating the risk area in acute coronary syndrome.

Non-Q-wave myocardial infarction

Between 30% and 50% of cases of myocardial infarction are considered to show non-Q-wave infarction. In general, myocardial disorders are slight and cardiac function is preserved in non-Q-wave infarction, compared with Q-wave infarction. Regarding prognosis, however, no differences have been reported between these diseases, and non-Q-wave infarction has been reported to have rather a high risk of leading to sudden cardiac death.

The rate of detection of non-Q-wave infarction using myocardial perfusion imaging is regarded to be roughly 50%, while it is also reportedly possible to identify the culprit coronary lesions using MIBG in nearly all cases. A comparative investigation into the detection of Q-wave and non-Q-wave infarction using ^{99m}Tc-sestamibi myocardial perfusion SPECT (MIBI) and MIBG SPECT [17] found that MIBI defects in non-Q-wave infarctions were significantly smaller than those in Q-wave infarctions, while no differences in MIBG defects were observed between the two types of infarction. In addition, the size of MIBG defects in Q-wave infarction was proportional to that of MIBI defects (i.e., the quantity of infarcted myocardium), while such a tendency was not observed in non-Q-wave infarction. In other words, in non-Q-wave infarction, a wide mismatch area is observed between perfusion SPECT and MIBG SPECT. This mismatch area is said to be denervated but viable (the plexus of sympathetic nerves has disappeared, but the viability of myocardial cells has been maintained), and is considered to be in an unstable state which easily results in lethal arrhythmia. This situation may be one of the reasons for the many cases of cardiac sudden death in non-Q-wave infarction.

Heart failure

Severity evaluation

It has been reported that the increased washout rate and the decreased H/M ratio on the delayed MIBG image become marked, with an increase in hypofunction in the left ventricle, in cases of heart failure, regardless of the underlying disease [18]. Similar results have been reported from studies on dilated cardiomyopathy (DCM) [19, 20], hypertrophic cardiomyopathy (HCM) [21], valvular heart disease [22, 23], pulmonary hypertension [24], amyloidosis [25], and diabetes [26]. As described above, the relationship between cardiac hypofunction and abnormal MIBG indices has been revealed in various diseases, and MIBG is thus useful for evaluation of the severity of heart failure. Figure 7 shows the correlation between the left ventricular ejection fraction (LVEF) and the washout rate of MIBG in patients with chronic heart failure.

According to a recent report [27], the H/M ratio on the delayed image and the washout rate correlated with brain natriuretic peptide, which is widely used as a marker for heart failure and heart-type fatty acid binding protein (H-FABP) and is attracting attention as a new marker for ongoing myocardial damage. In addition, another report indicated that the H/M ratio on the delayed image reflects the myocardial contractile reserve in patients with mild to moderate DCM [28].

Prognostic prediction

MIBG is also useful for prognostic evaluation in cases of heart failure. In 1992, in a study on DCM and ischemic

cardiomyopathy (ICM), Merlet et al. reported that patients with a lowered H/M ratio on the delayed MIBG image had an unfavorable prognosis and that the prognostic ability of MIBG imaging was superior to that of LVEF [29]. Subsequently, a large number of similar reports have appeared [30–35], and the H/M ratio on the delayed image and washout rate have been widely recognized as strong predictors of cardiac events in cases of heart failure, including DCM and ischemic heart diseases.

Regarding prognostics evaluation by MIBG, more detailed investigations have been undertaken, as described below. Imamura et al. [36] reported that application of background correction when calculating the washout rate improves its prognostic accuracy. Nakata et al. [37] reported that cases in which the H/M ratio was maintained on the delayed image had a favorable prognosis regardless of the washout rate, that cases in which the H/M ratio was lowered on the delayed image generally had an unfavorable prognosis, and that cases with a markedly lowered accumulation, even on the early image, had the most unfavorable prognosis. Kyuma et al. [38] reported that ability to predict the prognosis was improved by evaluating other factors, including the brain natriuretic peptide value and complications due to diabetes or kidney functional disorders, in addition to MIBG. Matsui et al. [39] and Fujimoto et al. [40] conducted MIBG myocardial scintigraphy before treatment and at 6 months after the start of treatment, and reported that the improvement rating was an excellent prognostic predictor.

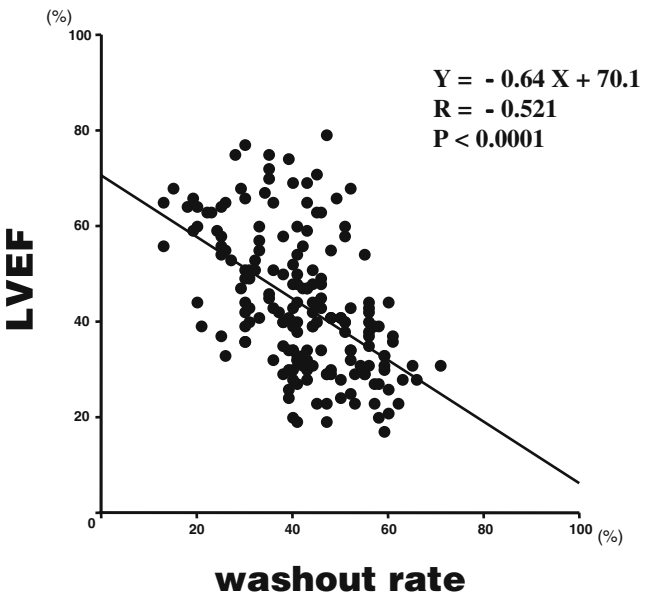

Fig. 7 Correlation between the washout rate of MIBG and LVEF in cases of chronic heart failure. In MIBG myocardial scintigraphy conducted 185 times in cases of chronic heart failure, the washout rate showed a significant negative correlation with the LVEF determined by echocardiography conducted during the same period. Cases with markedly lowered cardiac function tended to show higher washout rate values

Evaluation of the therapeutic effects of drugs

The effectiveness of β-blockers and angiotensin-converting enzyme inhibitors (ACE-Is) has been fully established in DCM. The use of MIBG before and after drug therapy has yielded an improvement in the washout rate and the H/M ratio on the delayed image, with an improvement in cardiac function, indicating its usefulness for the evaluation of therapeutic effects. Investigations have been conducted into the use of treatment with β-blockers [41–43], ACE-Is [44], spironolactone [45], and angiotensin receptor blockers (ARBs) [46, 47].

The efficacy of using two drugs has also been tentatively examined using MIBG, and there have been reports on carvedilol and metoprolol (β-blockers) [48, 49], perindopril and enalapril (ACE-Is) [50], and valsartan (ARB) and enalapril (ACE-I) [51].

Concerning diseases other than DCM, it has been reported that MIBG myocardial scintigraphy may be used to evaluate the usefulness of both nicorandil in ICM [52] and atrial natriuretic peptide in acute heart failure [53].

Prior prediction of therapeutic effects

Several studies have been conducted on whether it is possible to predict the effectiveness of β-blocker therapy for DCM based on the findings of MIBG myocardial scintigraphy. In each of these studies, ‘responders’ are patients showing an improvement in cardiac function to a certain degree or better, at a certain time point (at about 6 months) after the start of treatment. However, the results varied between studies, as follows: On the early image the retained cardiac accumulation and the washout rate showed no relationship to response to therapy [54]. The H/M ratio on the delayed image was significantly higher in responders [55]. Responders showed a low washout rate [56]. It was reported to be difficult to differentiate responders from non-responders, but possible to predict cases of β-blocker intolerance (exacerbations of heart failure) [57]. When an investigation was performed into the improvement of cardiac function for a relatively short period, as described above, no consensus was obtained regarding the usefulness of MIBG for the prediction of therapeutic effects.

Recently, an investigation was performed based on whether the long-term prognosis was improved by drug therapy. Nakata et al. [58] conducted a study in patients with heart failure, including ischemic heart diseases, treated with ACE-Is or β-blockers and found that the long-term prognosis was favorable in cases in which the H/M ratio on the delayed image was maintained on MIBG myocardial scintigraphy.

According to a report by Fujimoto et al. [59], the washout rate was improved by β-blocker therapy, and the long-term prognosis was favorable in cases with maintained accumulation on the early image and a high washout rate on MIBG myocardial scintigraphy conducted before the start of β-blocker therapy (Fig. 8, Table 1). Such cases are assumed to be in a state of hypertonia due to cardiac sympathetic nerves, but with maintenance of the integrity of the cardiac sympathetic nerve endings, indicating a group of cases highly likely to benefit from β-blocker therapy.

Usefulness of MIBG in HCM

MIBG is known to show decreased accumulation and increased washout at the site of myocardial hypertrophy in HCM. The H/M ratio and the washout rate correlate with the severity of the left ventricular systolic and diastolic dysfunction [60]. In addition, the H/M ratio correlates well with the left ventricular mass index and brain natriuretic peptide, while the washout rate also shows a good correlation with the serum norepinephrine concentration [21]. The H/M ratio correlates with the exercise tolerance [61], and the heterogeneity of MIBG accumulation correlates with the severity of cardiac hypofunction [62]. These reports support the usefulness of MIBG for evaluation of the severity of HCM.

Concerning the usefulness of MIBG for prognostic evaluation, it has been reported that the washout rate is increased significantly in cases showing ventricular tachyarrhythmia [63], and that the H/M ratio on the delayed image is a useful factor for predicting the development of heart failure in such cases [64].

Evaluation in cases after heart transplantation

In the experimentally prepared globally denervated canine heart, MIBG exhibited normal accumulation on the early image and was washed out on the delayed image, resulting in no accumulation. This state is due to a non-neuronal uptake mechanism referred to as uptake-2. On the other hand, in a human heart transplanted several months earlier, MIBG exhibited complete absence of accumulation, even on the early image [65]. This reflects the completely denervated state of the heart after transplantation, and demonstrates that uptake-2 does not participate in the dynamics of MIBG in the human heart.

It has been reported that MIBG exhibits no accumulation in the heart within 1 year after transplantation, and that the accumulation begins to recover at the anterobasal site with the subsequent course [66, 67], indicating the usefulness of MIBG in monitoring the course of sympathetic reinnervation in the transplanted heart.

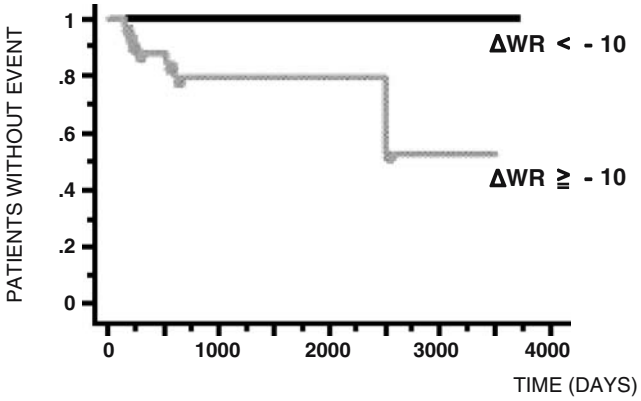

Fig. 8 Prediction of the therapeutic effectiveness of β-blockers by MIBG (from reference [59]). In 53 patients with dilated cardiomyopathy receiving β-blocker therapy continuously for 6 months or longer, MIBG myocardial scintigraphy was performed twice, before and 6–12 months afterthe start of the treatment. The improvement in the washout rate (*WR*) before and after treatment was the strongest prognostic predictor. No cardiac events occurred in the group of patients showing an improvement in washout rate by10% or more due to β-blocker therapy

In maze operation for atrial fibrillation, the cardiac sympathetic nerves are in a denervated state in the early phase after operation, but reinnervation is recognized in the chronic phase, according to a report on verification using MIBG [68].

Diseases other than ischemic heart diseases and heart failure

Arrhythmia

A high rate of MIBG abnormalities is observed in arrhythmogenic right ventricular cardiomyopathy, even in the absence of abnormal morphology or function in the left

Table 1 Comparison of clinical characteristics, MIBG data and echocardiographic findings in patients with and without washout rate improvement by β-blockertherapy (modified from reference [59]). Lower values of the extent score and higher values of the washout rate on the earlyimage were factors predicting washout rate improvement by the therapy

	WR unimproved	WR improved	*P* value
Patients	34	19	
Age (yrs)	57±12	55±9	NS
Gender (male %)	76.5	89.5	NS
MIBG data			
eEXT	36.8±21.6	21.8±16.9	<0.05
dEXT	43.7±27.5	34.6±26.3	NS
eSEV	47.4±41.5	22.1±31.7	<0.05
dSEV	74.1±69.4	50.8±68.9	NS
WR (%)	45.6±7.5	52.2±9.0	<0.01
Echocardiogram data			
LVEF	0.36±0.11	0.30±0.07	NS

Data are presented as the mean±SD
WR washout rate, *e* early, *d* delayed, *EXT* extent score, *SEV* severity score, *LVEF* left ventricular ejection fraction

ventricle; this suggests the usefulness of MIBG in the early diagnosis of this disease [69]. MIBG is regarded as showing abnormalities frequently in the left ventricular muscle (junction) connected to the right ventricle [70]. In addition, it has been reported that the site of decreased accumulation of MIBG is related to the origin of ventricular tachycardia [71]. Decreased accumulation of MIBG has also been observed at inferior and inferoseptal sites in idiopathic long QT syndrome [72] and Brugada syndrome [73].

MIBG abnormalities have been reported in various arrhythmic diseases, and future large-scale and more detailed studies are required regarding the frequency and characteristics of decreased MIBG accumulation, and the relationship between this appearance and arrhythmogenicity.

"Takotsubo" cardiomyopathy (transient left ventricular apical ballooning)

In this disease, the clinical symptoms and abnormal electrocardiogram suggest acute myocardial infarction, but coronary angiography reveals no stenosis. Left ventricular imaging reveals hypercontraction at the base of the left ventricle, with no contraction of the apical portion. This characteristic finding resembles the pot ("*tsubo*" in Japanese) used to capture an octopus ("*Tako*" in Japanese), and the disease has thus been designated as Takotsubo cardiomyopathy. Mental or physical stress frequently plays a role in the development of this disease. Abnormal wall motion of the left ventricle is reversible, and in general the disease is regarded as having a favorable prognosis. It is said to account for about 2% of cases suspected to represent ST-segment elevation infarcts, and most cases occur in postmenopausal women [74].

Nuclear medical examinations are useful for the evaluation of Takotsubo cardiomyopathy [75]. When performing myocardial SPECT, ^{99m}Tc-tetrofosmin, ^{123}I-BMIPP, and MIBG all yield a defect image with the apical portion as the core in the acute phase, which is inconsistent with a region dominated by the coronary artery, while the degree of the defect reflects the severity of the disease. Any such state in the acute phase is normalized in the chronic phase. Among the aforementioned three tracers, MIBG reveals the highest defect and shows a tendency to yield abnormal findings that persist in the long term. The etiology of this disease has not yet been clarified, although according to one report the MIBG findings suggest that the cause may be neurogenic myocardial stunning [76].

Diabetes

Neuropathy is one of the important complications in diabetes, and the relationship between MIBG abnormalities and neuropathy has been investigated by various authors [77–79]. According to these reports, MIBG abnormalities were observed at a high rate even in diabetic patients without a clinically obvious complication due to neuropathy, suggesting the existence of cardiac sympathetic disorders from the early stage. In cases complicated by neuropathy, MIBG abnormalities were more marked, reflecting the disease severity. Abnormal MIBG findings were observed at a high rate in the inferoposterior wall region, indicating a decreased accumulation and an increased washout.

Epalrestat (an aldose reductase inhibitor) and vitamin B_{12} are employed as therapeutic drugs for diabetic peripheral neuropathy. According to several reports, MIBG is useful for evaluating the efficacy of these drugs [80, 81].

Lewy body disease

In 1994, it was reported that patients with Parkinson's disease (PD) exhibited a complete absence of accumulation of MIBG in the heart [82]; this finding has stimulated increasing interest in the use of MIBG in the evaluation of nervous diseases. In recent years, it has been revealed clinically and neuropathologically that PD, dementia with Lewy bodies (DLB), and pure autonomic failure are overlapping diseases. Lewy body disease has thus become a general term for all three diseases [83].

Based on the information obtained thus far, the complete absence of accumulation of MIBG in the heart is considered to be a finding specific to Lewy body disease [84]. Accordingly, MIBG is expected to become a strong diagnostic tool for differentiation between PD and other parkinsonian syndromes, and between DLB and Alzheimer's disease in patients showing dementia. In a comparative investigation into MIBG findings in patients with PD or DLB in the early disease stage [85], DLB exhibited a significantly unfavorable accumulation in the heart compared with PD, suggesting that MIBG may be of value in early diagnosis as well.

Future problems

Problems regarding inter-institutional differences in MIBG quantitative indices

The H/M ratio and the washout rate are generally used as quantitative indices in MIBG myocardial scintigraphy. H/M ratio values show significant variation according to the imaging apparatus employed, and particularly according to the collimators used. This results in the problem of large differences in reference values between institutions. In an investigation by Nishimura et al. in 1997 into 49 institutions, the normal value for the H/M ratio varied widely, from 1.4 to 2.8 [86].

Table 2 Factors causing differences in the H/M ratio and the washout rate between institutions

Parameter	Influential factors
H/M ratio	Types of imaging apparatus (especially collimators) employed
	Method of setting ROIs (site, size, form)
Washout rate	Practice of background correction
	Imaging starting time for the delayed image
	Practice of correction for decay due to the physical half-life of ^{123}I

^{123}I has a photo-peak at 529 keV in addition to the peak at 159 keV which is used for imaging. The main reason for the variation in the H/M ratio is considered to be differences between collimators with regard to the amount of scattering component produced by 529-keV gamma rays that is included in the data obtained at 159 keV. As 529-keV ^{123}I gamma rays have a high transmittance, the image quality is markedly impaired by scattered rays when using low-energy collimators, as are widely employed in cardiac examinations. In order to solve such problems, use of a collimator modified for ^{123}I or a medium-energy collimator has been proposed, although such collimators are available at only a limited number of institutions. The ^{123}I dual-window method [87] was developed as a method of excluding scattered rays originating from 529-keV gamma rays, without the need for special hardware; its usefulness has been confirmed in clinical cases [88] although it is not routinely used in clinical practice. In addition to the above factors, Table 2 cites other factors causing inter-institutional differences in MIBG indices.

Establishment of evidence for MIBG

In 2005, a joint research team of the Japanese Circulation Society (JCS) published Guidelines for the Clinical Use of Cardiac Nuclear Medicine [89]. The indications for MIBG printed in the Guidelines are shown in Table 3. The usefulness of MIBG in many heart diseases, including heart failure, is widely recognized. However, the evidence level is C for each item, because most studies have been conducted in only a small number of cases at a single institution owing to differences between institutions regarding the quantitative indices for MIBG, as described above. Accordingly, it is difficult to establish evidence under the existing circumstances.

It is possible for MIBG to directly and quantitatively evaluate cardiac sympathetic functions at the myocardial level. Thus, this form of scintigraphy is a valuable modality not easily substituted by other methods. In order to solve the problems regarding the differences between institutions, it is necessary to make efforts to standardize the quantita-

Table 3 Class/evidence classifications for MIBG quoted from the Guidelines for the Clinical Use of Cardiac Nuclear Medicine (JCS 2005)

Parameter	Classification
Identification of denervated area in infarction and unstable angina	Class IIb, level C
Identification of ischemia in vasospastic angina	Class IIa′, level C
Autonomic neuropathy in diabetes	Class IIa′, level C
Severity evaluation of heart failure	Class I, level C
Prognostic evaluation of heart failure	Class I, level C
Evaluation of therapeutic effects on heart failure	Class IIa, level C
Prediction of therapeutic effects on heart failure	Class IIb, level C
Arrhythmic diseases	Class IIb, level C
Class classification for the usefulness of examinations	
I	There is evidence supporting usefulness, or there is a general consensus as to usefulness
IIa	Usefulness is likely, based on the evidence and opinions
IIa′	The evidence is insufficient, but there is a consensus regarding usefulness among experts in Japan
IIb	Usefulness is not sufficiently established, based on the evidence and opinions
III	There is evidence supporting uselessness and occasional untoward effects, or there is a general consensus as to uselessness
Evidence level classification	
A	Demonstrated in a number of multicenter randomized intervention studies including more than 400 cases, or demonstrated by meta-analyses
B	Demonstrated in a number of multicenter randomized intervention studies including less than 400 cases, well-designed comparative studies, or large-scale cohort studies
C	Not demonstrated in randomized intervention studies, but supported by a consensus among experts

tive values used, such as the H/M ratio and the washout rate. In addition, practical large-scale clinical studies need to be performed with the aim of establishing evidence for the usefulness of MIBG.

References

1. Wieland DM, Wu J, Brown LE, Mangner TJ, Swanson DP, Beierwaltes WH. Radiolabeled adrenergic neuron-blocking agents: adrenomedullary imaging with [^{131}I]iodobenzylguanidine. J Nucl Med 1980;21:349–53.
2. Tobes MC, Jaques S Jr, Wieland DM, Sisson JC. Effect of uptake-one inhibitors on the uptake of norepinephrine and metaiodobenzylguanidine. J Nucl Med 1985;26:897–907.
3. Nakajo M, Shimabukuro K, Yoshimura H, Yonekura R, Nakabeppu Y, Tanoue P, et al. Iodine-131 metaiodobenzylguanidine intra- and extravesicular accumulation in the rat heart. J Nucl Med 1986;27:84–9.
4. Sisson JC, Wieland DM, Sherman P, Mangner TJ, Tobes MC, Jacques S Jr. Metaiodobenzylguanidine as an index of the adrenergic nervous system integrity and function. J Nucl Med 1987;28:1620–4.
5. Wieland DM, Brown LE, Tobes MC, Rogers WL, Marsh DD, Mangner TJ, et al. Imaging the primate adrenal medulla with [^{123}I] and [^{131}I] meta-iodobenzylguanidine: concise communication. J Nucl Med 1981;22:358–64.
6. Wieland DM, Brown LE, Rogers WL, Worthington KC, Wu JL, Clinthorne NH, et al. Myocardial imaging with a radioiodinated norepinephrine storage analog. J Nucl Med 1981;22:22–31.
7. Solanki KK, Bomanji J, Moyes J, Mather SJ, Trainer PJ, Britton KE. A pharmacological guide to medicines which interfere with the biodistribution of radiolabelled meta-iodobenzylguanidine (MIBG). Nucl Med Commun 1992;13:513–21.
8. Gill JS, Hunter GJ, Gane G, Camm AJ. Heterogeneity of the human myocardial sympathetic innervation: in vivo demonstration by iodine 123-labeled meta-iodobenzylguanidine scintigraphy. Am Heart J 1993;126:390–8.
9. Estorch M, Carrió I, Berna L, Lopez-Pousa J, Torres G. Myocardial iodine-labeled metaiodobenzylguanidine 123 uptake relates to age. J Nucl Cardiol 1995;2:126–32.
10. Tsuchimochi S, Tamaki N, Tadamura E, Kawamoto M, Fujita T, Yonekura Y, et al. Age and gender differences in normal myocardial adrenergic neuronal function evaluated by iodine-123-MIBG imaging. J Nucl Med 1995;36:969–74.
11. Rabinovitch MA, Rose CP, Schwab AJ, Fitchett DH, Honos GN, Stewart JA, et al. A method of dynamic analysis of iodine-123-metaiodobenzylguanidine scintigrams in cardiac mechanical overload hypertrophy and failure. J Nucl Med 1993;34:589–600.
12. Somsen GA, Borm JJ, de Milliano PA, van Vlies B, Dubois EA, van Royen EA. Quantitation of myocardial iodine-123 MIBG uptake in SPET studies: a new approach using the left ventricular cavity and a blood sample as a reference. Eur J Nucl Med 1995;22:1149–54.
13. Taki J, Yasuhara S, Takamatsu T, Nakaji2ma K, Tatami R, Ishise S, et al. Value of iodine-123 metaiodobenzylguanidine scintigraphy in patients with vasospastic angina. Eur J Nucl Med 1998;25:229–34.
14. Sakata K, Iida K, Kudo M, Yoshida H, Doi O. Prognostic value of I-123 metaiodobenzylguanidine imaging in vasospastic angina without significant coronary stenosis. Circ J 2005;69:171–6.
15. Tsutsui H, Ando S, Fukai T, Kuroiwa M, Egashira K, Sasaki M, et al. Detection of angina-provoking coronary stenosis by resting iodine 123 metaiodobenzylguanidine scintigraphy in patients with unstable angina pectoris. Am Heart J 1995;129:708–15.
16. Matsunari I, Schricke U, Bengel FM, Haase HU, Barthel P, Schmidt G, et al. Extent of cardiac sympathetic neuronal damage is determined by the area of ischemia in patients with acute coronary syndromes. Circulation 2000;101:2579–85.
17. Simula S, Lakka T, Laitinen T, Remes J, Kettunen R, Kuikka J, et al. Cardiac adrenergic denervation in patients with non-Q-wave versus Q-wave myocardial infarction. Eur J Nucl Med 2000;27:816–21.
18. Imamura Y, Ando H, Mitsuoka W, Egashira S, Masaki H, Ashihara T, et al. Iodine-123 metaiodobenzylguanidine images reflect intense myocardial adrenergic nervous activity in congestive heart failure independent of underlying cause. J Am Coll Cardiol 1995;26:1594–9.
19. Schofer J, Spielmann R, Schuchert A, Weber K, Schluter M. Iodine-123 meta-iodobenzylguanidine scintigraphy: a noninvasive method to demonstrate myocardial adrenergic nervous system disintegrity in patients with idiopathic dilated cardiomyopathy. J Am Coll Cardiol 1988;12:1252–8.
20. Merlet P, Dubois-Rande JL, Adnot S, Bourguignon MH, Benvenuti C, Loisance D, et al. Myocardial beta-adrenergic desensitization and neuronal norepinephrine uptake function in idiopathic dilated cardiomyopathy. J Cardiovasc Pharmacol 1992;19:10–6.
21. Matsuo S, Nakamura Y, Tsutamoto T, Kinoshita M. Impairments of myocardial sympathetic activity may reflect the progression of myocardial damage or dysfunction in hypertrophic cardiomyopathy. J Nucl Cardiol 2002;9:407–12.
22. Imamura Y, Ando H, Ashihara T, Fukuyama T. Myocardial adrenergic nervous activity is intensified in patients with heart failure without left ventricular volume or pressure overload. J Am Coll Cardiol 1996;28:371–5.
23. Tsutsui H, Ando S, Kubota T, Kuroiwa-Matsumoto M, Egashira K, Sasaki M, et al. Abnormalities of cardiac sympathetic neuronal and left ventricular function in chronic mitral regurgitation: assessment by iodine-123 metaiodobenzylguanidine scintigraphy. Am J Card Imaging 1996;10:14–22.
24. Sakamaki F, Satoh T, Nagaya N, Kyotani S, Oya H, Nakanishi N, et al. Correlation between severity of pulmonary arterial hypertension and ^{123}I-metaiodobenzylguanidine left ventricular imaging. J Nucl Med 2000;41:1127–33.
25. Hongo M, Urushibata K, Kai R, Takahashi W, Koizumi T, Uchikawa S, et al. Iodine-123 metaiodobenzylguanidine scintigraphic analysis of myocardial sympathetic innervation in patients with AL (primary) amyloidosis. Am Heart J 2002;144:122–9.
26. Sugiyama T, Kurata C, Tawarahara K, Nakano T. Is abnormal iodine-123-MIBG kinetics associated with left ventricular dysfunction in patients with diabetes mellitus? J Nucl Cardiol 2000;7:562–8.
27. Arimoto T, Takeishi Y, Niizeki T, Koyama Y, Okuyama H, Nozaki N, et al. Ongoing myocardial damage relates to cardiac sympathetic nervous disintegrity in patients with heart failure. Ann Nucl Med 2005;19:535–40.
28. Ohshima S, Isobe S, Izawa H, Nanasato M, Ando A, Yamada A, et al. Cardiac sympathetic dysfunction correlates with abnormal myocardial contractile reserve in dilated cardiomyopathy patients. J Am Coll Cardiol 2005;46:2061–8.
29. Merlet P, Valette H, Dubois-Rande JL, Moyse D, Duboc D, Dove P, et al. Prognostic value of cardiac metaiodobenzylguanidine imaging in patients with heart failure. J Nucl Med 1992;33:471–7.
30. Nakata T, Miyamoto K, Doi A, Sasao H, Wakabayashi T, Kobayashi H, et al. Cardiac death prediction and impaired cardiac sympathetic innervation assessed by MIBG in patients with failing and nonfailing hearts. J Nucl Cardiol 1998;5:579–90.
31. Imamura Y, Fukuyama T, Mochizuki T, Miyagawa M, Watanabe K, Ehime MIBG Heart Failure Study Investigators. Prognostic

value of iodine-123-metaiodobenzylguanidine imaging and cardiac natriuretic peptide levels in patients with left ventricular dysfunction resulting from cardiomyopathy. Jpn Circ J 2001;65:155–60.
32. Wakabayashi T, Nakata T, Hashimoto A, Yuda S, Tsuchihashi K, Travin MI, et al. Assessment of underlying etiology and cardiac sympathetic innervation to identify patients at high risk of cardiac death. J Nucl Med 2001;42:1757–67.
33. Ogita H, Shimonagata T, Fukunami M, Kumagai K, Yamada T, Asano Y, et al. Prognostic significance of cardiac ^{123}I metaiodobenzylguanidine imaging for mortality and morbidity in patients with chronic heart failure: a prospective study. Heart 2001;86:656–60.
34. Ebina T, Takahashi N, Mitani I, Sumita S, Ishigami T, Ashino K, et al. Clinical implications of cardiac ^{123}I-meta-iodobenzylguanidine scintigraphy and cardiac natriuretic peptides in patients with heart disease. Nucl Med Commun 2002;23:795–801.
35. Yamada T, Shimonagata T, Fukunami M, Kumagai K, Ogita H, Hirata A, et al. Comparison of the prognostic value of cardiac iodine-123 metaiodobenzylguanidine imaging and heart rate variability in patients with chronic heart failure: a prospective study. J Am Coll Cardiol 2003;41:231–8.
36. Imamura Y, Fukuyama T. Prognostic value of myocardial MIBG scintigraphy findings in patients with cardiomyopathy—importance of background correction for quantification of MIBG activity. Ann Nucl Med 2002;16:387–93.
37. Nakata T, Wakabayashi T, Kyuma M, Takahashi T, Hashimoto A, Ogata H, et al. Prognostic implications of an initial loss of cardiac metaiodobenzylguanidine uptake and diabetes mellitus in patients with left ventricular dysfunction. J Card Fail 2003;9:113–21.
38. Kyuma M, Nakata T, Hashimoto A, Nagao K, Sasao H, Takahashi T, et al. Incremental prognostic implications of brain natriuretic peptide, cardiac sympathetic nerve innervation, and noncardiac disorders in patients with heart failure. J Nucl Med 2004;45:155–63.
39. Matsui T, Tsutamoto T, Maeda K, Kusukawa J, Kinoshita M. Prognostic value of repeated ^{123}I-metaiodobenzylguanidine imaging in patients with dilated cardiomyopathy with congestive heart failure before and after optimized treatments—comparison with neurohumoral factors. Circ J 2002;66:537–43.
40. Fujimoto S, Inoue A, Hisatake S, Yamashina S, Yamashina H, Nakano H, et al. Usefulness of meta-[^{123}I]iodobenzylguanidine myocardial scintigraphy for predicting cardiac events in patients with dilated cardiomyopathy who receive long-term beta blocker treatment. Nucl Med Commun 2005;26:97–102.
41. Agostini D, Belin A, Amar MH, Darlas Y, Hamon M, Grollier G, et al. Improvement of cardiac neuronal function after carvedilol treatment in dilated cardiomyopathy: a ^{123}I-MIBG scintigraphic study. J Nucl Med 2000;41:845–51.
42. Fujimura M, Yasumura Y, Ishida Y, Nakatani S, Komamura K, Yamagishi M, et al. Improvement in left ventricular function in response to carvedilol is accompanied by attenuation of neurohumoral activation in patients with dilated cardiomyopathy. J Card Fail 2000;6:3–10.
43. Lotze U, Kaepplinger S, Kober A, Richartz BM, Gottschild D, Figulla HR. Recovery of the cardiac adrenergic nervous system after long-term beta-blocker therapy in idiopathic dilated cardiomyopathy: assessment by increase in myocardial ^{123}I-metaiodobenzylguanidine uptake. J Nucl Med 2001;42:49–54.
44. Takeishi Y, Atsumi H, Fujiwara S, Takahashi K, Tomoike H. ACE inhibition reduces cardiac iodine-123-MIBG release in heart failure. J Nucl Med 1997;38:1085–9.
45. Kasama S, Toyama T, Kumakura H, Takayama Y, Ichikawa S, Suzuki T, et al. Effect of spironolactone on cardiac sympathetic nerve activity and left ventricular remodeling in patients with dilated cardiomyopathy. J Am Coll Cardiol 2003;41:574–81.
46. Kasama S, Toyama T, Kumakura H, Takayama Y, Ichikawa S, Suzuki T, et al. Addition of valsartan to an angiotensin-converting enzyme inhibitor improves cardiac sympathetic nerve activity and left ventricular function in patients with congestive heart failure. J Nucl Med 2003;44:884–90.
47. Kasama S, Toyama T, Kumakura H, Takayama Y, Ichikawa S, Suzuki T, et al. Effects of candesartan on cardiac sympathetic nerve activity in patients with congestive heart failure and preserved left ventricular ejection fraction. J Am Coll Cardiol 2005;45:661–7.
48. Hirooka K, Yasumura Y, Ishida Y, Hanatani A, Nakatani S, Komamura K, et al. Comparative left ventricular functional and neurohumoral effects of chronic treatment with carvedilol versus metoprolol in patients with dilated cardiomyopathy. Jpn Circ J 2001;65:931–6.
49. Toyama T, Hoshizaki H, Seki R, Isobe N, Adachi H, Naito S, et al. Efficacy of carvedilol treatment on cardiac function and cardiac sympathetic nerve activity in patients with dilated cardiomyopathy: comparison with metoprolol therapy. J Nucl Med 2003;44:1604–11.
50. Kasama S, Toyama T, Kumakura H, Takayama Y, Ichikawa S, Suzuki T, et al. Effects of perindopril on cardiac sympathetic nerve activity in patients with congestive heart failure: comparison with enalapril. Eur J Nucl Med Mol Imaging 2005;32:964–71.
51. Kasama S, Toyama T, Hatori T, Sumino H, Kumakura H, Takayama Y, et al. Comparative effects of valsartan and enalapril on cardiac sympathetic nerve activity and plasma brain natriuretic peptide in patients with congestive heart failure. Heart 2006;92:625–30.
52. Kasama S, Toyama T, Hatori T, Kumakura H, Takayama Y, Ichikawa S, et al. Comparative effects of nicorandil with isosorbide mononitrate on cardiac sympathetic nerve activity and left ventricular function in patients with ischemic cardiomyopathy. Am Heart J 2005;150:477e1–e8.
53. Kasama S, Toyama T, Kumakura H, Takayama Y, Ishikawa T, Ichikawa S, et al. Effects of intravenous atrial natriuretic peptide on cardiac sympathetic nerve activity in patients with decompensated congestive heart failure. J Nucl Med 2004;45:1108–13.
54. Yamazaki J, Muto H, Kabano T, Yamashina S, Nanjo S, Inoue A. Evaluation of beta-blocker therapy in patients with dilated cardiomyopathy—clinical meaning of iodine 123-metaiodobenzylguanidine myocardial single-photon emission computed tomography. Am Heart J 2001;141:645–52.
55. Suwa M, Otake Y, Moriguchi A, Ito T, Hirota Y, Kawamura K, et al. Iodine-123 metaiodobenzylguanidine myocardial scintigraphy for prediction of response to beta-blocker therapy in patients with dilated cardiomyopathy. Am Heart J 1997;133:353–8.
56. Choi JY, Lee KH, Hong KP, Kim BT, Seo JD, Lee WR, et al. Iodine-123 MIBG imaging before treatment of heart failure with carvedilol to predict improvement of left ventricular function and exercise capacity. J Nucl Cardiol 2001;8:4–9.
57. Kakuchi H, Sasaki T, Ishida Y, Komamura K, Miyatake K. Clinical usefulness of ^{123}I meta-iodobenzylguanidine imaging in predicting the effectiveness of beta blockers for patients with idiopathic dilated cardiomyopathy before and soon after treatment. Heart 1999;81:148–52.
58. Nakata T, Wakabayashi T, Kyuma M, Takahashi T, Tsuchihashi K, Shimamoto K. Cardiac metaiodobenzylguanidine activity can predict the long-term efficacy of angiotensin-converting enzyme inhibitors and/or beta-adrenoceptor blockers in patients with heart failure. Eur J Nucl Med Mol Imaging 2005;32:186–94.
59. Fujimoto S, Inoue A, Hisatake S, Yamashina S, Yamashina H, Nakano H, et al. Usefulness of ^{123}I-metaiodobenzylguanidine myocardial scintigraphy for predicting the effectiveness of beta-blockers in patients with dilated cardiomyopathy from the

standpoint of long-term prognosis. Eur J Nucl Med Mol Imaging 2004;31:1356–61.
60. Terai H, Shimizu M, Ino H, Yamaguchi M, Uchiyama K, Oe K, et al. Changes in cardiac sympathetic nerve innervation and activity in pathophysiologic transition from typical to end-stage hypertrophic cardiomyopathy. J Nucl Med 2003;44:1612–7.
61. Isobe S, Izawa H, Iwase M, Nanasato M, Nonokawa M, Ando A, et al. Cardiac ^{123}I-MIBG reflects left ventricular functional reserve in patients with nonobstructive hypertrophic cardiomyopathy. J Nucl Med 2005;46:909–16.
62. Shimizu M, Ino H, Yamaguchi M, Terai H, Hayashi K, Nakajima K, et al. Heterogeneity of cardiac sympathetic nerve activity and systolic dysfunction in patients with hypertrophic cardiomyopathy. J Nucl Med 2002;43:15–20.
63. Terai H, Shimizu M, Ino H, Yamaguchi M, Hayashi K, Sakata K, et al. Cardiac sympathetic nerve activity in patients with hypertrophic cardiomyopathy with malignant ventricular tachyarrhythmias. J Nucl Cardiol 2003;10:304–10.
64. Hiasa G, Hamada M, Saeki H, Ogimoto A, Ohtsuka T, Hara Y, et al. Cardiac sympathetic nerve activity can detect congestive heart failure sensitively in patients with hypertrophic cardiomyopathy. Chest 2004;126:679–86.
65. Dae MW, De Marco T, Botvinick EH, O'Connell JW, Hattner RS, Huberty JP, et al. Scintigraphic assessment of MIBG uptake in globally denervated human and canine hearts—implications for clinical studies. J Nucl Med 1992;33:1444–50.
66. De Marco T, Dae M, Yuen-Green MS, Kumar S, Sudhir K, Keith F, et al. Iodine-123 metaiodobenzylguanidine scintigraphic assessment of the transplanted human heart: evidence for late reinnervation. J Am Coll Cardiol 1995;25:927–31.
67. Guertner C, Krause BJ, Klepzig H Jr, Herrmann G, Lelbach S, Vockert EK, et al. Sympathetic re-innervation after heart transplantation: dual-isotope neurotransmitter scintigraphy, norepinephrine content and histological examination. Eur J Nucl Med 1995;22:443–52.
68. Mabuchi M, Imamura M, Kubo N, Morita K, Noriyasu K, Tsukamoto T, et al. Sympathetic denervation and reinnervation after the maze procedure. J Nucl Med 2005;46:1089–94.
69. Takahashi N, Ishida Y, Maeno M, Hirose Y, Kawano S, Fukuoka S, et al. Noninvasive identification of left ventricular involvements in arrhythmogenic right ventricular dysplasia: comparison of ^{123}I-MIBG, ^{201}TlCl, magnetic resonance imaging and ultrafast computed tomography. Ann Nucl Med 1997;11:233–41.
70. Lerch H, Bartenstein P, Wichter T, Hindricks G, Borggrefe M, Breithardt G, et al. Sympathetic innervation of the left ventricle is impaired in arrhythmogenic right ventricular disease. Eur J Nucl Med 1993;20:207–12.
71. Wichter T, Hindricks G, Lerch H, Bartenstein P, Borggrefe M, Schober O, et al. Regional myocardial sympathetic dysinnervation in arrhythmogenic right ventricular cardiomyopathy. An analysis using ^{123}I-meta-iodobenzylguanidine scintigraphy. Circulation 1994;89:667–83.
72. Gohl K, Feistel H, Weikl A, Bachmann K, Wolf F. Congenital myocardial sympathetic dysinnervation (CMSD)—a structural defect of idiopathic long QT syndrome. Pacing Clin Electrophysiol 1991;14:1544–53.
73. Wichter T, Matheja P, Eckardt L, Kies P, Schafers K, Schulze-Bahr E, et al. Cardiac autonomic dysfunction in Brugada syndrome. Circulation 2002;105:702–6.
74. Gianni M, Dentali F, Grandi AM, Sumner G, Hiralal R, Lonn E. Apical ballooning syndrome or takotsubo cardiomyopathy: a systematic review. Eur Heart J 2006;27:1523–9.
75. Ito K, Sugihara H, Kinoshita N, Azuma A, Matsubara H. Assessment of Takotsubo cardiomyopathy (transient left ventricular apical ballooning) using ^{99m}Tc-tetrofosmin, ^{123}I-BMIPP, ^{123}I-MIBG and ^{99m}Tc-PYP myocardial SPECT. Ann Nucl Med 2005;19:435–45.
76. Akashi YJ, Nakazawa K, Sakakibara M, Miyake F, Musha H, Sasaka K. ^{123}I-MIBG myocardial scintigraphy in patients with "takotsubo" cardiomyopathy. J Nucl Med 2004;45:1121–7.
77. Hattori N, Tamaki N, Hayashi T, Masuda I, Kudoh T, Tateno M, et al. Regional abnormality of iodine-123-MIBG in diabetic hearts. J Nucl Med 1996;37:1985–90.
78. Giordano A, Calcagni ML, Verrillo A, Pellegrinotti M, Frontoni S, Spallone V, et al. Assessment of sympathetic innervation of the heart in diabetes mellitus using ^{123}I-MIBG. Diabetes Nutr Metab 2000;13:350–5.
79. Schnell O, Hammer K, Muhr-Becker D, Ziegler A, Weiss M, Tatsch K, et al. Cardiac sympathetic dysinnervation in type 2 diabetes mellitus with and without ECG-based cardiac autonomic neuropathy. J Diabetes Complications 2002;16:220–7.
80. Utsunomiya K, Narabayashi I, Tamura K, Nakatani Y, Saika Y, Onishi S, et al. Effects of aldose reductase inhibitor and vitamin B12 on myocardial uptake of iodine-123 metaiodobenzylguanidine in patients with non-insulin-dependent diabetes mellitus. Eur J Nucl Med 1998;25:1643–8.
81. Utsunomiya K, Narabayashi I, Nakatani Y, Tamura K, Onishi S. I-123 MIBG cardiac imaging in diabetic neuropathy before and after epalrestat therapy. Clin Nucl Med 1999;24:418–20.
82. Hakusui S, Yasuda T, Yanagi T, Takahashi A, Hasegawa Y, Inoue M. ^{123}I-MIBG myocardial scintigraphical analysis in patients with and without autonomic disorder. Clin Neurol 1994;34:402–4.
83. Hishikawa N, Hashizume Y, Yoshida M, Sobue G. Clinical and neuropathological correlates of Lewy body disease. Acta Neuropathol (Berl) 2003;105:341–50.
84. Taki J, Yoshita M, Yamada M, Tonami N. Significance of ^{123}I-MIBG scintigraphy as a pathophysiological indicator in the assessment of Parkinson's disease and related disorders: it can be a specific marker for Lewy body disease. Ann Nucl Med 2004;18:453–61.
85. Suzuki M, Kurita A, Hashimoto M, Fukumitsu N, Abo M, Ito Y, et al. Impaired myocardial ^{123}I-metaiodobenzylguanidine uptake in Lewy body disease: comparison between dementia with Lewy bodies and Parkinson's disease. J Neurol Sci 2006;240:15–9.
86. Nishimura T, Sugishita Y, Sasaki Y. The results of questionnaire on quantitative assessment of ^{123}I-metaiodobenzylguanidine myocardial scintigraphy in heart failure. Kaku Igaku 1997;34:1139–48.
87. Motomura N, Ichihara T, Takayama T, Aoki S, Kubo H, Takeda K. Practical compensation method of downscattered component due to high energy photon in ^{123}I imaging. Kaku Igaku 1999;36:997–1005.
88. Kobayashi H, Momose M, Kanaya S, Kondo C, Kusakabe K, Mitsuhashi N. Scatter correction by two–window method standardizes cardiac I-123 MIBG uptake in various gamma camera systems. Ann Nucl Med 2003;17:309–13.
89. Tamaki N, Kusakabe K, Kubo A, Kumazaki T, Shimamoto K, Senda S, et al. Guidelines for clinical use of cardiac nuclear medicine (JSC2005). Circ J 2005;69 Suppl 4:1125–202.